Title: Lower Energy Excitation of Water Soluble Near-Infrared Emitting Mixed-Ligand Metallacrowns

Authors: Tu Ngoc Nguyen; Svetlana V. Eliseeva; Ivana Martinić; Peggy L. Carver; Stéphane Petoud; Vincent L. Pecoraro

To be cited as: 10.1002/chem.202300226

Link to VoR: https://doi.org/10.1002/chem.202300226

COMMUNICATION

Lower Energy Excitation of Water Soluble Near-Infrared Emitting Mixed-Ligand Metallacrowns

Tu N. Nguyen,[a, d] Svetlana V. Eliseeva,*[b] Ivana Martinić,[b] Peggy L. Carver,[c] Timothée Lathion,[a] Stéphane Petoud,*[b] Vincent L. Pecoraro*[a]

[a] Dr. T. N. Nguyen,[+] Prof. V. L. Pecoraro
Department of Chemistry, Willard H. Dow Laboratories
University of Michigan
Ann Arbor, Michigan 48109 (USA)
E-mail: vlpec@umich.edu
URL: https://lsa.umich.edu/chem/people/faculty/vlpec.html

[b] Dr. S.V. Eliseeva,[+] Dr. I. Martinić, Prof. S. Petoud
Centre de Biophysique Moléculaire, CNRS UPR 4301
Rue Charles Sadron, 45071 Orléans Cedex 2 (France)
Email: svetlana.eliseeva@cnrs-orleans.fr; stephane.petoud@inserm.fr
URL : http://cbm-petoud.cnrs-orleans.fr/

[c] Prof. P.Carver
College of Pharmacy and Michigan Medicine
University of Michigan
Ann Arbor, Michigan 48109 (USA)

[d] Dr. T. N. Nguyen[+]
Present address: Helen Scientific Research and Technological Development Co., Ltd,
Ho Chi Minh City (Vietnam)

[+] These authors contributed equally.

Supporting information for this article is given via a link at the end of the document.

Abstract: By combining advantages of two series of lanthanide(III)/zinc(II) metallacrowns (MCs) assembled using pyrazine- ($pyzHA^{2-}$) and quinoxaline- ($quinoHA^{2-}$) hydroximate building blocks ligands, we created here water-soluble mixed-ligand MCs with extended absorption to the visible range. The Yb^{III} analogue demonstrated improved photophysical properties in the near-infrared (NIR) range in cell culture media, facilitating its application for NIR optical imaging in living HeLa cells.

Introduction

In vivo optical imaging in the near-infrared (NIR) region (650–1700 nm) enables us to peer deeply within living objects and provides unique information for clinical diagnosis or for biological research.[1] However, to generate high-resolution and high-contrast images, luminescent probes with specific functional properties are required.[2] Single-walled carbon nanotubes (SWCTs), quantum dots (QDs), small organic molecules, silica or polymer nanoparticles (NPs) loaded with organic dyes, as well as inorganic NPs have been prepared and tested.[3] Nanomaterial probes can be harmful because of long-term retention times and unidentified toxicity, causing safety issues for clinical applications. Small organic fluorophores are potential molecular probes with low toxicity. However, their use is often limited because of the decay of their fluorescence signal due to the decomposition of the molecule upon exposure to the excitation light (photobleaching). Also, the production of organic fluorophores often requires long and difficult multistep synthesis. As an alternative providing complementary advantages, NIR-emitting molecular compounds incorporating lanthanide(III) (Ln^{III}) ions have been suggested.[4] The unique optical properties of Ln^{III} ions include sharp emission bands the wavelength positions of which are unaffected by experimental conditions. In addition, Ln^{III} compounds are highly photostable, making them very attractive for optical biological imaging. However, the design of molecular probes incorporating Ln^{III} ions able to generate a sufficiently high signal intensity from Ln^{III} f-f transitions in the NIR range under biological conditions, remains challenging. [4a, 5] First, the low molar absorption coefficients of free Ln^{III} ions that are due to the forbidden nature of most f-f transitions need to be overcome. This goal can be reached by locating in sufficiently close proximity to the Ln^{III} appropriate chromophores able to absorb large amounts of excitation light and to transfer the resulting energy to the accepting levels of Ln^{III} in order to sensitize them ('antenna effect').[6] Secondly, to limit the non-radiative deactivation of the excited states of Ln^{III} through overtones of O-H, N-H or CH vibrations, a specific ligand design is required to create a protective environment around the Ln^{III} and to prevent a direct coordination of solvent molecules.[5a, 5c] In addition, for use in biological conditions, molecular luminescent probes should be biocompatible and excitable using low energy light to prevent damages to cells and tissues.

To address these challenges, our group has created a family of photostable Ln^{III}/Zn^{II} metallacrowns (MCs) with unique 'encapsulated sandwich' structures that efficiently protect Ln^{III} from non-radiative deactivations and sensitize characteristic NIR emissions of Yb^{III}, Nd^{III} and Er^{III} ions. $Zn_{16}Ln(HA)_{16}$ were assembled using picoline- ($picHA^{2-}$),[7] pyrazine- ($pyzHA^{2-}$),[8] quinaldine- ($quinHA^{2-}$),[9] napthyridine- ($napHA^{2-}$)[10] and quinoxaline- ($quinoHA^{2-}$)[10] hydroximate building blocks ligands. With this approach, absorption bands have been shifted from the UV to the visible domain when going from $Zn_{16}Ln(picHA)_{16}$ to $Zn_{16}Ln(quinoHA)_{16}$. Moreover, the Ln^{III}-centered photophysical

properties of $Zn_{16}Ln(HA)_{16}$ can be finely tuned by the choice of the hydroximate ligands.[10] However, only $Zn_{16}Ln(pyzHA)_{16}$ MCs, which exhibit absorption in the UV range, proved to be sufficiently water soluble and therefore suitable for biological applications. We have previously shown that $Zn_{16}Ln(pyzHA)_{16}$ behaves well when placed with living HeLa cells demonstrating viability values superior to 90% upon incubation with concentrations up to 45 µM of MC for 24 and 48 h. We have also assessed minimal inhibitory concentration (MIC) of $Zn_{16}Ln(pyzHA)_{16}$ against microbes such as *Escherichia coli* (MIC: 250 µg/mL), *Staphylococcus aureus* (MIC: 125 µg/mL) and *Candida albicans* (MIC: 2000 µg/mL), for which it displays minimal toxicity (see Supporting Information). The $Zn_{16}Ln(pyzHA)_{16}$ MC has been shown to be able to differentiate necrotic and living HeLa cells and label selectively the former.[8] We also shown that this MC can be utilized for combined *in vitro* cell fixation and counter staining with NIR signal.[11] Nevertheless, UV sensitization of Ln^{III} NIR emission in $Zn_{16}Ln(pyzHA)_{16}$ is less desirable for optical imaging due to the strong interaction of such excitation light with biological materials and could significantly limit a range of potential applications. Therefore, the shift of absorption/excitation bands towards longer wavelengths would be advantageous. This operation often requires the use of large organic chromophores with extended conjugation that tend to be more hydrophobic and therefore would diminishes the water-solubility of the MCs.

Herein, we present an innovative approach to modulate the functional properties of Ln^{III}/Zn^{II} MCs by creating mixed-ligand $Zn_{16}Ln(pyzHA)_x(quinoHA)_{16-x}$ (Ln = Nd, Yb, Er; x = 15–7). This approach combines uniquely the advantages of both types of MCs, in particular, extended to the visible range absorption bands of $Zn_{16}Ln(quinoHA)_{16}$ with the hydrophilicity and biocompatibility of $Zn_{16}Ln(pyzHA)_{16}$.

Results and Discussion

$Zn_{16}Ln(HA)_{16}$ MCs are usually obtained by a self-assembly reaction between Zn^{II} and Ln^{III} triflates with the corresponding hydroxamic acid in a 16:2:16 molar ratio.[8-9] The use of an excess (2 equivalents) amount of Ln^{III} salt ensures the formation of pure products. To synthesize mixed-ligand MCs, H_2pyzHA and H_2quinoHA were introduced in an aqueous solution with a 12:4 molar ratio in the presence of pyridine (py), followed by the addition of 16 and 2 equivalents of $Zn(OTf)_2$ and $Ln(OTf)_3$, respectively. Crystals of $[Zn_{16}Ln(pyzHA)_x(quinoHA)_{16-x}(py)_8](OTf)_3$ (shortland $Zn_{16}Ln(pyzHA)_x(quinoHA)_{16-x}$, Ln = Nd, Er, Yb) were formed in three days and collected by filtration. Mass-spectrometry analysis of $Zn_{16}Ln(pyzHA)_x(quinoHA)_{16-x}$ performed in a positive mode in water revealed the formation of different species with x ranging from 15 to 7 (Figure 1, Supporting Information). Moreover, it was found that the composition of the main species is dependent on the nature of the Ln^{III}. In the mass spectrum of the Nd^{III} MC, the most intense peaks correspond to $[Zn_{16}Nd(pyzHA)_{11}(quinoHA)_5]^{3+}$ and $[Zn_{16}Nd(pyzHA)_{10}(quinoHA)_6]^{3+}$ species (x = 11 and 10), while in those of the MCs formed with Yb^{III} and Er^{III}, the main species are $[Zn_{16}Ln(pyzHA)_{13}(quinoHA)_3]^{3+}$ and $[Zn_{16}Ln(pyzHA)_{12}(quinoHA)_4]^{3+}$ (x = 13 and 12). Such behavior can be caused by the differences in the coordination kinetics of the reaction. Indeed, analysis of the crystal structures (Supporting Information)[8, 10] revealed that the O–Yb–O angles are essentially the same (70.6°) for $Zn_{16}Yb(pyzHA)_{16}$ and $Zn_{16}Yb(quinoHA)_{16}$, suggesting that $pyzHA^{2-}$ and $quinoHA^{2-}$ coordinate kinetically to Yb^{III} in a similar way. Therefore, the composition of the main species present in the mass spectra of the MC formed with Yb^{III} is consistent with the $pyzHA^{2-}/quinoHA^{2-}$ ratio initially introduced into the self-assembly reaction. In the case of Nd^{III} MCs, the O–Nd–O angle decreases from 69.4° for $Zn_{16}Nd(pyzHA)_{16}$ to 65.1° for $Zn_{16}Nd(quinoHA)_{16}$, reflecting potential differences in the coordination kinetics of $pyzHA^{2-}$ and $quinoHA^{2-}$ ligands with Nd^{III}. As a consequence, the main MC species formed with Nd^{III} may not correspond to the ratio between the hydroximate ligands that was used for the synthesis. Moreover, the larger Nd^{III} ion can accommodate more ligands and/or ligands of larger size, i.e. $quinoHA^{2-}$, so that $[Zn_{16}Nd(pyzHA)_{11}(quinoHA)_5]^{3+}$ and $[Zn_{16}Nd(pyzHA)_{10}(quinoHA)_6]^{3+}$ are the main species, their peaks dominating the mass-spectrum of $Zn_{16}Nd(pyzHA)_x(quinoHA)_{16-x}$. The polydispersity index (PDI) calculated from the mass-spectral distribution (Supporting Information) is independent of the nature of the Ln^{III} and equal to 1 for all synthesized mixed-ligand MCs. The values of the average molecular weights for Nd^{III}, Er^{III} and Yb^{III} MCs are 4734, 4664 and 4681 g/mol, respectively, that corresponds to the following formulae $[Zn_{16}Nd(pyzHA)_{10.6}(quinoHA)_{5.4}(py)_8](OTf)_3$, $[Zn_{16}Er(pyzHA)_{12.5}(quinoHA)_{3.5}(py)_8](OTf)_3$ and $[Zn_{16}Yb(pyzHA)_{12.2}(quinoHA)_{3.8}(py)_8](OTf)_3$. All of the synthesized $Zn_{16}Ln(pyzHA)_x(quinoHA)_{16-x}$ (Ln = Nd, Er, Yb) MCs proved soluble in water and Opti-MEM cell culture medium at least up to a concentration of 25 mg/mL. In addition, we have demonstrated previously the long-term stability of $Zn_{16}Ln(pyzHA)_{16}$[8] and $Zn_{16}Ln(quinoHA)_{16}$[10] in solution (over one month) in water or methanol, respectively, by mass-spectrometry and ^{1}H NMR. It is worth noting that when the proportion of H_2quinoHA is increased, e.g. the molar ratio of H_2pyzHA:H_2quinoHA being 8:8 or 4:12, the obtained MCs are mainly insoluble in water, suggesting that a majority of $pyzHA^{2-}$ in the MC is necessary, and the 12:4 molar ratio of hydroxamic acids introduced into the reactions is adequate.

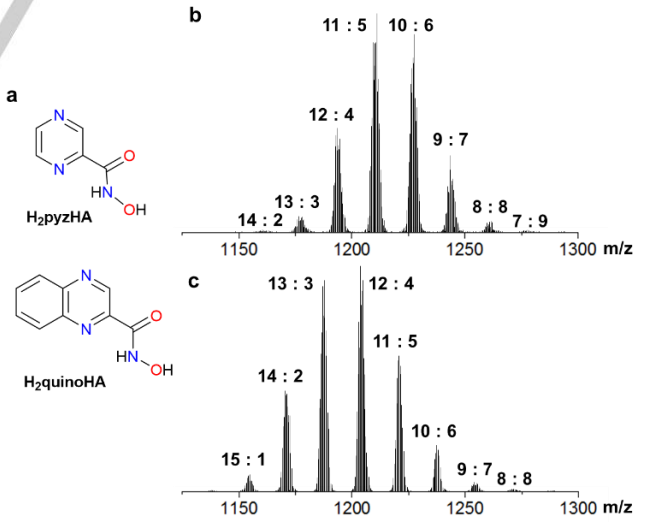

Figure 1. (a) Structural formulae of hydroxamic acids. Mass-spectra of (b) $[Zn_{16}Nd(pyzHA)_x(quinoHA)_{16-x}]^{3+}$ and (c) $[Zn_{16}Yb(pyzHA)_x(quinoHA)_{16-x}]^{3+}$ collected in water showing the presence of species with different ratios $pyzHA^{2-}$: $quinoHA^{2-}$ (x : (16–x)).

Absorption spectra were acquired for solutions of $Zn_{16}Ln(pyzHA)_x(quinoHA)_{16-x}$ in water and compared with those of $Zn_{16}Ln(quinoHA)_{16}$ in methanol and $Zn_{16}Ln(pyzHA)_{16}$ in water

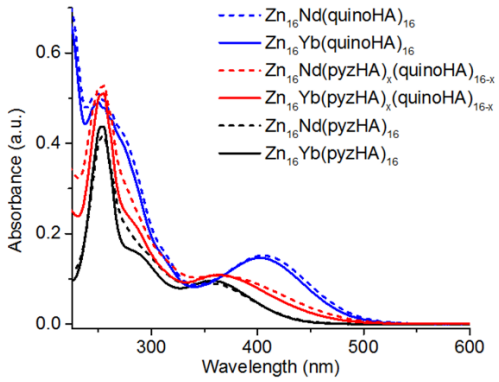

Figure 2. Absorption spectra of $Zn_{16}Ln(pyzHA)_{16}$ (2 µM, H_2O), $Zn_{16}Ln(pyzHA)_x(quinoHA)_{16-x}$ (10 µg/mL, H_2O) and $Zn_{16}Ln(quinoHA)_{16}$ (2 µM, CH_3OH), room temperature.

(Figure 2). They exhibit broad bands typical of $Zn_{16}Ln(HA)_{16}$ MCs, due to π→π* transitions in the UV range and a band arising from an intra-ligand charge-transfer (ILCT) at longer wavelengths. The presence of this ILCT band is specific for $Zn_{16}Ln(HA)_{16}$ MCs and suggests that $Zn_{16}Ln(pyzHA)_x(quinoHA)_{16-x}$ remain intact in solution in water at 10 µg/mL concentration. It was shown that the formation of the mixed-ligand MCs results in an extension of the low-energy ILCT band towards the visible range, up to 500 nm, with a significantly larger absorption at wavelengths longer than 400 nm compared to that of $Zn_{16}Ln(pyzHA)_{16}$.

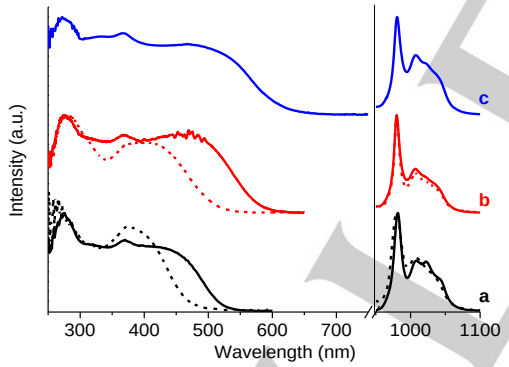

Figure 3. (Left) Excitation spectra upon monitoring Yb^{III} emission at 980 nm. (Right) Emission spectra under excitation at 370–470 nm. (a) $Zn_{16}Yb(pyzHA)_{16}$;[8, 11] (b) $Zn_{16}Yb(pyzHA)_x(quinoHA)_{16-x}$; (c) $Zn_{16}Yb(quinoHA)_{16}$.[10] Solid lines: samples in the solid state; dashed lines: solutions in Opti-MEM + 2% FBS, *c* = 150 µM for $Zn_{16}Yb(pyzHA)_{16}$ and 500 µg/mL for $Zn_{16}Yb(pyzHA)_x(quinoHA)_{16-x}$.

Photophysical properties of the most luminescent Yb^{III} analogue were studied in the solid state and in solution in Opti-MEM cell culture medium supplemented with 2 % fetal bovine serum (FBS) to better mimic subsequent cell imaging experiments (*vide infra*). Upon monitoring the emission signal at 980 nm that arises from Yb^{III}, excitation spectra of $Zn_{16}Yb(pyzHA)_x(quinoHA)_{16-x}$ present broad ligand-centered bands in the UV-visible range (Figure 3, left, red traces). As the Yb^{III} ion doesn't possess any electronic transition in the visible range, these spectra demonstrate that the sensitization of Yb^{III} luminescence is occurring through the electronic states of the MC scaffold. Moreover, the presence of the low-energy ILCT band in the range of 340–500 nm indicates that $Zn_{16}Yb(pyzHA)_x(quinoHA)_{16-x}$ remain intact in Opti-MEM cell culture medium supplemented with 2% FBS at 500 µg/mL concentration.

The shape of the excitation spectrum of $Zn_{16}Yb(pyzHA)_x(quinoHA)_{16-x}$ collected in solution matches the shape of the absorption spectrum (Figure 2, red traces) while the excitation spectra recorded on sample in the solid state exhibits signals extended up to 600 nm. The latter can be explained by saturation effects.[12] The comparison of the excitation spectra of the mixed-ligand Yb^{III} MC with those of $Zn_{16}Yb(pyzHA)_{16}$ and $Zn_{16}Yb(quinoHA)_{16}$ revealed the same trend as shown for the absorption spectra, i.e. a red and a blue shift compared to the former and the latter, respectively. The excitation into the ILCT bands of $Zn_{16}Yb(pyzHA)_x(quinoHA)_{16-x}$ in the solid state and in solution results in the generation of the characteristic Yb^{III} emission in the NIR range centered at 980 nm, arising from the $^2F_{5/2}\rightarrow{}^2F_{7/2}$ transition (Figure 3, right, red traces).

Table 1. Yb^{III}-centered quantum yields under ligands excitation (Q^L_{Yb}) and luminescence lifetimes (τ_{obs}) for $Zn_{16}Yb(HA)_{16}$.[a]

HA	State	Q^L_{Yb} (%)[b]	τ_{obs} (µs)[c]
pyzHA/quinoHA	Solid	0.426(7)	37.0(2)
	Opti-MEM + 2% FBS	$5.4(3)\cdot10^{-2}$	10.9(3) : 40% 26.0(8) : 60%
pyzHA[d]	Solid	0.659(4)	45.6(3)
	Opti-MEM + 2% FBS	$1.25(1)\cdot10^{-2}$	6.45(5): 89% 24(1): 11%
quinoHA[e]	Solid	0.637(5)	49.7(2)

[a] Data collected at room temperature. Concentrations of solutions are 150 µM for $Zn_{16}Yb(pyzHA)_{16}$ and 500 µg/mL for $Zn_{16}Yb(pyzHA)_x(quinoHA)_{16-x}$. Standard deviation ($2\sigma$) between parentheses; estimated relative errors: τ_{obs}, ±2%; Q^L_{Yb}, ±10 %. [b] Under excitation at 320–420 nm. [c] Under excitation at 355 nm. [d] From Refs. [8, 11]. [e] From Ref. [10].

Yb^{III}-centered absolute quantum yield values measured under excitation into the ligands bands (Q^L_{Yb}) for the samples in the solid state are ~1.5-times lower for $Zn_{16}Yb(pyzHA)_x(quinoHA)_{16-x}$ compared to those of $Zn_{16}Yb(pyzHA)_{16}$ and $Zn_{16}Yb(quinoHA)_{16}$ (Table). Luminescence decay of the mixed-ligand MC collected upon monitoring the emission signal arising from the Yb^{III} $^2F_{5/2}$ level is monoexponential for the sample in the solid state. This result reflects the similarity of the coordination environments around the emissive Yb^{III} ion despite the presence of MCs formed with different ratios of $pyzHA^{2-}$ and $quinoHA^{2-}$ ligands (Figure 1c). The corresponding observed lifetime (τ_{obs}) values are slightly (1.2–1.3 times) shorter for the mixed-ligand MC *vs*. those of $Zn_{16}Yb(pyzHA)_{16}$ and $Zn_{16}Yb(quinoHA)_{16}$. Such behavior could reflect the presence of additional sources of non-radiative deactivation of Yb^{III} through co-crystallized solvent molecules. On the other hand, for solutions of Yb^{III} MCs analyzed in cell culture media, the values of Q^L_{Yb} are 4.3-times larger for the mixed-ligand MC in comparison to $Zn_{16}Yb(pyzHA)_{16}$ and the average value of τ_{obs} is 1.9-times longer (23(1) µs for the mixed-ligand MC *vs*. 12(1)

µs) for $Zn_{16}Yb(pyzHA)_{16}$. It should be noted that luminescence decays of $Zn_{16}Yb(pyzHA)_x(quinoHA)_{16-x}$ are bi-exponential in solution. The same trend was previously observed for $Zn_{16}Ln(pyzHA)_{16}$ and was attributed to the existence of emissive Ln^{III} MCs possessing two different microenvironments caused by the presence of (bio)molecules in cell culture media.[11]

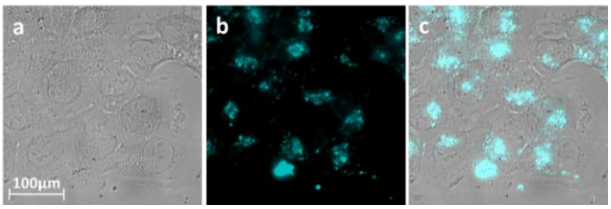

Figure 4. Images obtained from epifluorescence microscopy experiments performed on HeLa cells incubated with a 500 µg/mL solution of $Zn_{16}Yb(pyzHA)_x(quinoHA)_{16-x}$ during 3h. (a) Brightfield image. (b) NIR emission (λ_{ex}: 447 nm band pass 60 nm filter, λ_{em}: long pass 805 nm filter, exposure time: 5 s). (c) Merged (a) and (b) images. 63× objective.

NIR epifluorescence microscopy experiments were performed on living HeLa cells incubated with 500 µg/mL solution of $Zn_{16}Yb(pyzHA)_x(quinoHA)_{16-x}$ in Opti-MEM cell culture medium supplemented with 2% FBS during 3 h (Figure 4). A NIR emission signal arising from the Yb^{III} mixed-ligand MC was detected with a 805 nm long-pass filter under excitation with light selected by a 447 band pass 60 nm filter. The granular pattern observed on the NIR microscopy images suggests that the mixed-ligand MCs are able to be taken up by living HeLa cells and indicate their localization in cytoplasmic vesicles. Such behavior contrasts with that observed for $Zn_{16}Ln(pyzHA)_{16}$ that exhibited an ability to preferentially accumulate in necrotic cells while not penetrating into living ones.[8]

Conclusions

In summary, we have demonstrated the validity of an innovative mixed-ligand approach to fine-tune functional properties of MCs by creating $Zn_{16}Ln(pyzHA)_x(quinoHA)_{16-x}$ (Ln = Nd, Yb, Er; x = 15–7). The obtained MCs synergistically combine advantages of both hydroximate ligands and possess a water solubility associated with enhanced absorption in the visible range. Moreover, for the Yb^{III} analogue, the sensitization range is extended towards lower energy, to 600 nm for the sample in the solid state. $Zn_{16}Yb(pyzHA)_x(quinoHA)_{16-x}$ in cell culture media exhibits ~4-times improved NIR luminescence quantum yield and ~2-fold longer observed average lifetime. Finally, Yb^{III} emission in the NIR is maintained under biological conditions and has been successfully used for NIR epifluorescence imaging experiments of living HeLa cells. This work opens new perspectives for further smart modulation of functional properties of Ln^{III}-based coordination compounds.

Experimental Section

Reagents and methods. All manipulations were performed under aerobic conditions using chemicals and solvents as received unless otherwise stated. ESI-MS spectra were collected with a Micromass LCT time-of-flight electrospray mass spectrometer in negative ion mode at a cone voltage of −40 V on samples dissolved in water. Samples were injected via a syringe pump. Data were processed with the program MassLynx 4.0.

Synthesis of $[Zn_{16}Ln(pyzHA)_x(quinoHA)_{16-x}(py)_8](OTf)_3$ ($Zn_{16}Ln(pyzHA)_x(quinoHA)_{16-x}$, Ln = Nd, Er, Yb). A general synthetic procedure for these compounds is described below for the Nd^{III} analogue. Complexes formed with other Ln^{III} were prepared in the same way by using corresponding amounts of $Ln(OTf)_3$. H_2pyzHA and H_2quinoHA were synthesized according to synthetic procedures described previously.[8, 10] H_2pyzHA (37.6 mg, 0.27 mmol) and H_2quinoHA (17.0 mg, 0.09 mmol) were added into a solution containing 1.0 mL of pyridine and 5.0 mL of H_2O. The solution was stirred for 5 minutes until the solids were completely dissolved. $Zn(OTf)_2$ (130.5 mg, 0.36 mmol) and $Nd(OTf)_3$ (26.6 mg, 0.045 mmol) were added, the resulting orange solution was stirred for 5 minutes and then filtered. The filtrate was kept undisturbed to give orange crystals after 2-3 days. The crystals, triflate salts of MCs with the general composition $[Zn_{16}Nd(pyzHA)_x(quinoHA)_{16-x}(py)_8](OTf)_3$ were collected by filtration and dried in air. Yield ~30 mg.

ESI-MS mass-spectra performed on $Zn_{16}Ln(pyzHA)_x(quinoHA)_{16-x}$ (Ln = Nd, Er, Yb) are provided in Supporting Information.

Details about the synthesis and characterization of $Zn_{16}Ln(pyzHA)_{16}$ and $Zn_{16}Ln(quinoHA)_{16}$ are provided in Refs.[8, 10]

Photophysical measurements. Data were collected on samples in the solid state or for freshly prepared solutions placed into 2.4 mm i.d. quartz capillaries or quartz Suprasil cells. Absorption spectra were acquired on a Cary 100Bio spectrophotometer. Steady-state emission and excitation spectra were measured on a Horiba-Jobin-Yvon Fluorolog 3 spectrofluorimeter equipped with a visible photomultiplier tube (PMT) (220-800 nm, R928P; Hamamatsu) and a NIR PMT (950-1650 nm, H10330-75; Hamamatsu). All spectra were corrected for the instrumental functions. Luminescence lifetimes were determined under excitation at 355 nm provided by a Nd:YAG laser (YG 980; Quantel), the signals in the NIR range were detected by the H10330-75 PMT connected to the iHR320 monochromator (Horiba Scientific). The output signals from the detectors were fed into a 500 MHz bandpass digital oscilloscope (TDS 754C; Tektronix) and transferred to a PC for data processing with the Origin 8® software. Luminescence lifetimes are averages of three or more independent measurements. Quantum yields were determined with a Fluorolog 3 spectrofluorimeter based on the absolute method using an integration sphere (GMP SA, see Supporting Information for details). Each sample was measured several times varying the position of samples. Estimated experimental error for the determination of quantum yields is ~10%.

HeLa cells culture and epifluorescence microscopy experiments. The HeLa (Human Cervical Carcinoma Cells) cell line obtained from ATCC (Molsheim, France) was cultured in Dulbecco's modified Eagle's medium (DMEM) supplemented with 10% heat-inactivated fetal bovine serum (FBS, purchased from Sigma F7524), 1% of 100× non-essential amino acid solution (Sigma M7145), 1% of L-glutamine (GlutaMAX) and 1% of streptomycin/penicilin antibiotics (Sigma P4333). Cells were seeded in a 8-well Lab Tek Chamber coverglass (Nunc, Dutsher S.A., Brumath, France) at a density of $6{\cdot}10^4$ cells/well and cultured at 37°C in a 5% humidified CO_2 atmosphere. After 24h, the cell culture medium was removed, cells were washed twice with Opti-MEM reduced serum medium (room temperature) and

incubated with a 500 µg/mL solution of $Zn_{16}Yb(pyzHA)_x(quinoHA)_{16-x}$ in Opti-MEM medium (supplemented with 2% of FBS at 37°C in a 5% CO_2 atmosphere) during 3h. Prior to the epifluorescence imaging, cells were washed twice with Opti-MEM (room temperature). Obtained cells were observed with a Zeiss Axio Observer Z1 fluorescence inverted microscope (Zeiss, Le Pecq, France) equipped with an EMCCD Photometrics Evolve 512 (Roper Scientific) camera. The Zeiss HXP 120 white light source was used in combination with the following filter cubes: (i) 447 nm band pass 60 nm for the excitation and a long pass 805 nm filter to monitor the Yb^{III} emission in the NIR range. A 63× Plan-Apochromat objective was used for these experiments.

Acknowledgements

This research was supported in part by the National Science Foundation under grant CHE-1664964, La Ligue Contre le Cancer, the Réseau 'Molécules Marines, Métabolisme & Cancer' du Cancéropôle Grand Ouest and La Région Centre. S.P. acknowledges support from Institut National de la Santé et de la Recherche Médicale (INSERM).

Conflicts of interest

S.P. and V.L.P. are founders of the bioimaging company VIEWaves.

Keywords: metallacrown • lanthanide • near-infrared • luminescence • optical imaging

[1] a)B. R. Smith, S. S. Gambhir, *Chem. Rev.* **2017**, *117*, 901-986; b)S. He, J. Song, J. Qu, Z. Cheng, *Chem. Soc. Rev.* **2018**, *47*, 4258-4278; c)Kenry, Y. Duan, B. Liu, *Adv. Mater.* **2018**, *30*, e1802394; d)Q. Miao, K. Pu, *Adv. Mater.* **2018**, *30*, e1801778; e)C. Wang, Z. Wang, T. Zhao, Y. Li, G. Huang, B. D. Sumer, J. Gao, *Biomat.* **2018**, *157*, 62-75.

[2] G. Chen, I. Roy, C. Yang, P. N. Prasad, *Chem. Rev.* **2016**, *116*, 2826-2885.

[3] a)Y. Cai, Z. Wei, C. Song, C. Tang, W. Han, X. Dong, *Chem. Soc. Rev.* **2019**, *48*, 22-37; b)J. Xu, A. Gulzar, P. Yang, H. Bi, D. Yang, S. Gai, F. He, J. Lin, B. Xing, D. Jin, *Coord. Chem. Rev.* **2019**, *381*, 104-134; c)Y. Fan, F. Zhang, *Adv. Opt. Mater.* **2019**, *7*, 1801417; d)I. Martinić, S. V. Eliseeva, S. Petoud, *J. Lumin.* **2017**, *189*, 19-43.

[4] a)Y. Y. Ning, M. L. Zhu, J. L. Zhang, *Coord. Chem. Rev.* **2019**, *399*, 213028; b)G.-Q. Jin, Y. Ning, J.-X. Geng, Z.-F. Jiang, Y. Wang, J.-L. Zhang, *Inorg. Chem. Front.* **2020**, *7*, 289-299; c)J.-C. G. Bünzli, *Chem. Rev.* **2010**, *110*, 2729-2755; d)S. V. Eliseeva, J.-C. G. Bünzli, *Chem. Soc. Rev.* **2010**, *39*, 189-227.

[5] a)S. Comby, J.-C. G. Bünzli, in *Handbook on the Physics and Chemistry of Rare Earths, Vol. 37, Ch. 235* (Eds.: K. A. Gschneidner Jr., J.-C. G. Bünzli, V. K. Pecharsky), Elsevier Science B.V., Amsterdam, **2007**, pp. 217-470; b)I. Hernández, W. P. Gillin, in *Handbook on the Physics and Chemistry of Rare Earths, Vol. 47* (Eds.: J.-C. G. Bünzli, V. K. Pecharsky), Elsevier, **2015**, pp. 1-100; c)J.-C. G. Bünzli, S. V. Eliseeva, in *Comprehensive Inorganic Chemistry II, Vol. 8* (Ed.: V. W.-W. Yam), Elsevier B.V., Amsterdam, **2013**, pp. 339-398; d)G.-Q. Jin, C. V. Chau, J. F. Arambula, S. Gao, J. L. Sessler, J.-L. Zhang, *Chem. Soc. Rev.* **2022**, *51*, 6177-6209; e)J.-Y. Hu, Y. Ning, Y.-S. Meng, J. Zhang, Z.-Y. Wu, S. Gao, J.-L. Zhang, *Chem. Sci.* **2017**, *8*, 2702-2709; f)Y. Ning, J. Tang, Y.-W. Liu, J. Jing, Y. Sun, J.-L. Zhang, *Chem. Sci.* **2018**, *9*, 3742-3753; g)Y. Ning, Y.-W. Liu, Z.-S. Yang, Y. Yao, L. Kang, J. L. Sessler, J.-L. Zhang, *J. Am. Chem. Soc.* **2020**, *142*, 6761-6768.

[6] a)Y. Hasegawa, Y. Kitagawa, T. Nakanishi, *NPG Asia Materials* **2018**, *10*, 52-70; b)H. Uh, S. Petoud, *Comptes Rendus Chimie* **2010**, *13*, 668-680.

[7] J. Jankolovits, C. M. Andolina, J. W. Kampf, K. N. Raymond, V. L. Pecoraro, *Angew. Chem. Int. Ed.* **2011**, *50*, 9660-9664.

[8] I. Martinić, S. V. Eliseeva, T. N. Nguyen, V. L. Pecoraro, S. Petoud, *J. Am. Chem. Soc.* **2017**, *139*, 8388-8391.

[9] E. R. Trivedi, S. V. Eliseeva, J. Jankolovits, M. M. Olmstead, S. Petoud, V. L. Pecoraro, *J. Am. Chem. Soc.* **2014**, *136*, 1526-1534.

[10] S. V. Eliseeva, T. N. Nguyen, J. W. Kampf, E. R. Trivedi, V. L. Pecoraro, S. Petoud, *Chem. Sci.* **2022**, *13*, 2919-2931.

[11] I. Martinić, S. V. Eliseeva, T. N. Nguyen, F. Foucher, D. Gosset, F. Westall, V. L. Pecoraro, S. Petoud, *Chem. Sci.* **2017**, *8*, 6042-6050.

[12] a)H. Wei, Z. Zhao, C. Wei, G. Yu, Z. Liu, B. Zhang, J. Bian, Z. Bian, C. Huang, *Adv. Func. Mater.* **2016**, *26*, 2085-2096; b)M. Ganapathi, S. V. Eliseeva, N. R. Brooks, D. Soccol, J. Fransaer, K. Binnemans, *J. Mater. Chem.* **2012**, *22*, 5514-5522.

Entry for the Table of Contents

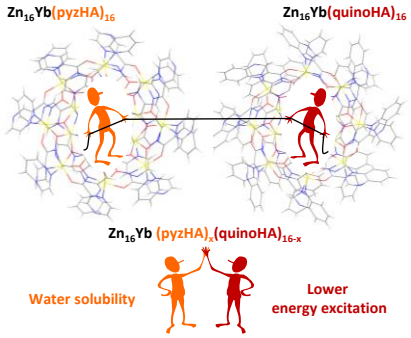

Water solubility of $Zn_{16}Ln(pyzHA)_{16}$ (H_2pyzHA: pyrazine hydroxamic acid) or lower energy excitation of $Zn_{16}Ln(quinoHA)_{16}$ (H_2quinoHA: quinoxaline hydroxamic acid) metallacrowns (MCs)? No need to choose! In water soluble mixed-ligand $Zn_{16}Yb(pyzHA)_x(quinoHA)_{16-x}$ MCs characteristic emission of Yb^{III} in the near-infrared range can be sensitized upon excitation up to 600 nm in the solid state or 500 nm in aqueous solution.